

---

# GENERALIZATION OF GRAPH NETWORK INFERENCES IN HIGHER-ORDER PROBABILISTIC GRAPHICAL MODELS

---

A PREPRINT

**Yicheng Fei**  
Rice University  
Houston, TX 77005  
yf17@rice.edu

**Xaq Pitkow**  
Baylor College of Medicine  
Rice University  
Center for Neuroscience and Artificial Intelligence  
Houston, TX 77030  
xaq@rice.edu

July 14, 2021

## ABSTRACT

Probabilistic graphical models provide a powerful tool to describe complex statistical structure, with many real-world applications in science and engineering from controlling robotic arms to understanding neuronal computations. A major challenge for these graphical models is that inferences such as marginalization are intractable for general graphs. These inferences are often approximated by a distributed message-passing algorithm such as Belief Propagation, which does not always perform well on graphs with cycles, nor can it always be easily specified for complex continuous probability distributions. Such difficulties arise frequently in expressive graphical models that include intractable higher-order interactions. In this paper we construct iterative message-passing algorithms using Graph Neural Networks defined on factor graphs to achieve fast approximate inference on graphical models that involve many-variable interactions. Experimental results on several families of graphical models demonstrate the out-of-distribution generalization capability of our method to different sized graphs, and indicate the domain in which our method gains advantage over Belief Propagation.

## 1 Introduction

To draw conclusions about individual variables of interest in a task, one builds structured probabilistic graphical models to describe statistical relations among all variables and marginalizes out all other unobserved variables. Such exact inference computations are infeasible in general, due to exponential complexity in practice when the latent space is large. Often the latent space to be marginalized is decomposable due to conditional independencies between variables, allowing us to represent the full distribution as a probabilistic graphical model (PGM) [1]. This may allow us to perform difficult global calculations using simpler integrations on subsets of variables. Such approaches are used by message-passing algorithms like Belief Propagation (BP) [2] and Expectation Propagation (EP) [3], widely used approaches to computing or approximating marginal probabilities using distributed computation. BP is guaranteed to yield exact results if the graph has a tree structure. However, on general graphs with loops, which are likely to be better descriptors of real data, BP can give approximate posteriors or even fail to converge.

Graphical models with pairwise interactions like Hopfield network [4] and Boltzmann machine [5] have provided us with intriguing models for memory and learning, and has developed to layered neural networks which are widely used nowadays. However, sometimes basic pairwise interaction models do not suffice to explain real data patterns like neuronal avalanches [6], retinal activity patterns when exposing to natural stimuli [7], and simultaneous silence of cultured hippocampal neurons [8]. Taking one step further, structured third-order interactions have been proposed for general probabilistic models [9], and have been used to model conditional correlation structure in movies [10]. Including higher-order interactions increases model flexibility, but the number of possible interactions grows combinatorially with the interaction order. This makes exact inference problems intractable with limited computational resources and numbers of data points. Thus prior knowledge like locality or sparsity of interactions must be used, resulting in a

structured factor graph. Higher-order factor graph may have more loops compared to a pairwise graph with as many interactions. Local message-passing algorithms like BP suffer in the presence of loops and are thus likely to perform worse on many real-world graphical models. Even when applied to higher-order trees, message updates for BP usually don't have closed-form solutions, so running BP on these graphs becomes impractical.

To mitigate these drawbacks of BP and to provide an alternative on loopy graphs even without analytical update formulas, in this work we present a method to learn a recursive message-passing algorithm for fast approximate inference. Our method applies to a large family of higher-order graphical models with a wide range of graph structures and parameter values including very loopy ones. In the spirit of BP, we use a Graph Neural Network (GNN) [11, 12] to perform message-passing on factor graphs. We train this network to compute sufficient statistics of all univariate marginal distributions simultaneously for each instance sampled from a parametrized family of PGMs.

To study the performance of our method, we perform experiments on two artificial datasets where we can calculate ground truth, and compare performance to BP: Gaussian Graphical Models (GGM) and a small binary spin-glass system with third-order interactions. GGMs only have pairwise interactions, but the ground truth marginals can easily be computed without message-passing for very large graphs. The graph size is kept under 15 for the binary spin-glass dataset for exact calculation of marginal probabilities by enumeration [13]. In addition, we construct a dataset of continuous PGMs with pairwise and third-order interactions. Since closed-form marginals do not exist for this interesting model class, we train our model to predict univariate statistics calculated by Markov Chain Monte Carlo (MCMC) sampling.

Our experiments show that the learnt algorithm has better performance than BP on an in-distribution test dataset, even when excluding those graphs on which BP dynamics don't converge. We also show that our model generalizes reliably out of distribution to probabilistic graphical models of different sizes than the training set. By looking at the error distribution for two graph metrics—average shortest path length and cluster coefficient—we find that our method outperforms BP particularly well on graphs with small average shortest path length and large cluster coefficients, which are the properties of many real world graphs [14]. This suggests there is potential for using our model as an approximation inference method on real-world PGMs with higher-order interactions.

## 2 Related Work

Previous work has explored learning to pass messages that calculate marginal probabilities in graphical models. Some examined fast and approximate calculation of Belief Propagation or Expectation Propagation updates when analytical integration is not feasible for computing on the level of single factor [15, 16, 17]. Others created message-passing algorithms for inference in probabilistic graphical models, trying to learn an algorithm that is more accurate than Belief Propagation when the underlying graph is loopy [13]. The most related work to ours uses stacked bi-directional GNNs on factor graphs to perform maximum *a posteriori* estimation on binary graphical models [18]. One major difference is that we use a recurrent network instead of a feedforward one, so our method uses far fewer parameters and scales to larger graphs without adding new layers. Another difference is that we incorporate an attentional mechanism [19] to increase model flexibility. Another related study puts a factor graph NN layer within a recurrent algorithm to calculate marginal probabilities in binary graphical models, applying them to low density parity check codes and Ising models [20]. Instead of using a GNN to learn a novel message-passing algorithm from scratch, the authors build their algorithm on top of Belief Propagation and let GNN serve as an error-correction module for loopy BP.

Traditional Graph Neural Networks are defined on regular graphs with nodes and edges, and thus best work with models with only pairwise interactions. On the other hand, factor graphs or hypergraphs, which represent higher-order interactions directly, are usually preferred for message-passing algorithms like BP. Factor graphs [21] use two types of nodes: variable nodes (circles) for each variable, and factor nodes (squares) for each subset of directly interacting variables; edges connect factors to their constituent variables. Some work has been done to extend GNNs to such higher-order graphs [22, 23], including studies aiming to solve graph isomorphism tasks [24], and others applying GNNs to data living on simplicial complexes [25].

## 3 Methods

### 3.1 Probabilistic Graphical Models and Factor Graphs

Probabilistic graphical models describe the conditional dependence structure among random variables using graphs. We describe higher-order interactions using a factor graph [21], which expresses the joint probability density as a product of local factors,  $p(\mathbf{x}) \propto \prod_i f_i(\mathbf{x}_i)$ , each involving only a subset of variables  $\mathbf{x}_i$ . Exact inference in tree graphs can be performed by iteratively marginalizing out the leaves of the tree and propagating this information along the graph. This

iterative algorithm is called belief propagation (BP), and has been applied with some success even on graphs with loops [2, 26]. Message updates in BP include multivariate integration, and don't always have close-form solutions. (Fully factorized) Expectation Propagation (EP) [3] is an approximation to mitigate this issue by projecting the outgoing message to some user-chosen parametric family.

### 3.2 Graph Neural Networks

Graph Neural Networks (GNN) are artificial neural networks implementing a message-passing operation on a graph [11]. A GNN updates each node's representation based on aggregated messages from its neighbours. Each node  $i$  represents information as a vector  $\mathbf{h}_i^t$  that evolves over time (or layer)  $t$ , and edges are assigned a vector weight  $\mathbf{e}_{ij}$ . The updated representation at time/layer  $t + 1$  can be described by:

$$\mathbf{h}_i^{t+1} = \mathcal{U} \left( \mathbf{h}_i^t, \bigsqcup_{j \in N(i) \setminus \{j\}} \mathcal{M}(\mathbf{h}_j^t, \mathbf{h}_i^t, \mathbf{e}_{ij}) \right) \quad (1)$$

where every message  $\mathcal{M}(\mathbf{h}_j^t, \mathbf{h}_i^t, \mathbf{e}_{ij})$  from neighbour  $j$  to node  $i$  along edge  $ij$  is first calculated using a common trainable nonlinear function  $\mathcal{M}$ , then messages from all neighbours are aggregated together by a permutation-invariant function  $\bigsqcup$  (e.g. summation), before being used to update each target node through another trainable function  $\mathcal{U}$ . We recommend [27] for a review of methods and application of GNNs.

### 3.3 Factor Graph Neural Network

In order to implement a message-passing algorithm on factor graphs, we first define a Graph Neural Network on bipartite graphs, unlike a typical GNN that treats all nodes equally [28, 29, 12]. We thus define two distinct node types for variables and factors, represented by hidden vectors  $\mathbf{h}_{v,i}^{(t)}$  and  $\mathbf{h}_{f,i}^{(t)}$ , with corresponding message and update functions for each. We also augment our GNN functions with a few extra operations. We reasoned that it would be beneficial if our network could identify loops and re-weight incoming messages accordingly, since Belief Propagation [2, 30] applied to loopy graphs exhibits errors traced back to the assumption of independent neighbors. To this end we use the attention mechanism [19] when aggregating message functions and we update hidden node representations using Gated Recurrent Unit (GRU) [31] with LayerNorm [32] to imbue nodes with a long-term memory. In summary, our iterative algorithm is an RNN, with the activation layer being a bi-directional graph neural network with self-attention, as described mathematically below.

Our target inferences are over graphical models within the exponential family [33, 34], a broad class of probability distributions widely used in statistical analysis. The density of such a distribution can be parameterized by a vector of natural parameters  $\boldsymbol{\eta}$ :

$$p(\mathbf{x}) = \frac{1}{Z(\boldsymbol{\eta})} \exp(\boldsymbol{\eta}^\top \mathbf{T}(\mathbf{x})) \quad (2)$$

where  $\mathbf{T}(\mathbf{x})$  is the vector of sufficient statistics and  $Z(\boldsymbol{\eta})$  is a normalization constant. Combined with the factorization of the joint density, each individual factor can also be parametrized with its own vector of natural parameters  $\boldsymbol{\eta}_i$ :

$$p(\mathbf{x}) = \frac{1}{Z(\boldsymbol{\eta})} \prod_i \exp(\boldsymbol{\eta}_i^\top \mathbf{T}_i(\mathbf{x}_i)) \quad (3)$$

A PGM is then represented by sets of factor nodes, variable nodes, edges, and all natural parameters,  $\{\mathcal{F}, \mathcal{V}, \mathcal{E}, H\}$ . The process of marginalization converts the natural parameters to expectation parameters [35, 1].

We use a MultiLayer Perceptron (MLP) to initialize the hidden states for factor nodes based on the natural parameters of the target graphical model. Separate MLPs are used for different types of factors, e.g., pairwise factors and third-order factors. The hidden states for variable nodes are initialized as a zero vector.

$$\mathbf{h}_{f,i}^{(0)} = \text{Encoder1}(\boldsymbol{\eta}_f) \quad (4)$$

$$\mathbf{h}_{v,j}^{(0)} = \mathbf{0} \quad (5)$$

After initialization, we then update each node's hidden representation recurrently for  $N$  time steps. In each step, a bi-directional Graph Attention Network (GAT) [19] layer is used to calculate messages and they are aggregated as the activation for a GRU unit to compute the hidden state for the next step. Separate multi-head GAT networks are used for two types of messages: from variable node to factor node, and from factor node to variable node. Likewise, we use different trainable weights for different factor types since they may behave differently. For the factor node updates,

we take a similar approach as in [36] and transform the aggregated incoming message from neighboring variables by a factor-specific feature matrix  $\mathbf{F}_i \in \mathbb{R}^{H \times H}$  as a constant input, which is mapped from its natural parameter  $\boldsymbol{\eta}_i$  by a shared MLP for each type of factors.

$$\mathbf{F}_i = \text{Encoder2}(\boldsymbol{\eta}_i) \quad (6)$$

The following equations show one-step message-passing for factor nodes. The updates for variable nodes are similar except for that there is no variable node feature, so eq. (10) is replaced by  $\mathbf{a}_i^{(t+1)} = \mathbf{m}_i^{(t+1)}$ . eqs. (7) and (8) reflect only one attention head. For multi-head attention, we simply duplicate  $M_{f \leftarrow v}$  and  $W_{f \leftarrow v}$  modules and the multi-head weighted summation in eq. (9) is averaged over all heads. In our experiments, we use 5 attention heads for smoother learning.

$$\text{raw message from variable } j \text{ to factor } i: \quad \mathbf{m}_{f \leftarrow v, ij}^{(t+1)} = M_{f \leftarrow v}(\mathbf{h}_{f,i}^{(t)}, \mathbf{h}_{v,j}^{(t)}) \quad (7)$$

$$\text{attention weight from variable } j \text{ to factor } i: \quad \alpha_{f \leftarrow v, ij}^{(t+1)} = \frac{W_{f \leftarrow v}(\mathbf{h}_{f,i}^{(t)}, \mathbf{h}_{v,j}^{(t)})}{\sum_{k \in N(i)} W_{f \leftarrow v}(\mathbf{h}_{f,i}^{(t)}, \mathbf{h}_{v,k}^{(t)})} \quad (8)$$

$$\text{weighted summary message from variable } j \text{ to factor } i: \quad \mathbf{m}_i^{(t+1)} = \sum_{k \in N(i)} \alpha_{f \leftarrow v, ik}^{(t+1)} \mathbf{m}_{f \leftarrow v, ik}^{(t+1)} \quad (9)$$

$$\text{incorporate local factor features:} \quad \mathbf{a}_i^{(t+1)} = \mathbf{F}_i \mathbf{m}_i^{(t+1)} \quad (10)$$

$$\text{update hidden state of factor } i: \quad \mathbf{h}_{f,i}^{(t+1)} = \text{GRU}_f(\mathbf{a}_i^{(t+1)}, \mathbf{h}_{f,i}^{(t)}) \quad (11)$$

We would like our model to learn an iterative algorithm that converges to the target. So instead of choosing the number of time steps  $N$  to be fixed, which we found often yielded RNN dynamics that passed through the target output without stopping, we randomly sample a readout time  $N$  from a range, so the network cannot rely on any particular readout time. At that point we use a decoder MLP to read out expectation parameters of the univariate marginal distributions for each variable:

$$\mathbf{y}_j = \text{Decoder}(\mathbf{h}_{v,j}^{(N)}) \quad (12)$$

### 3.4 Datasets

There are two practical use cases for applying our methods to improve on BP. First is to improve inference accuracy on loopy graphs where BP starts to perform poorly, and second is to make fast but approximate inferences on PGMs for which algorithms like BP or even Expectation Propagation [3] become infeasible to run.

For tractability, most probabilistic models are based on pairwise interactions. But pairwise models would require many nonlinear auxiliary hidden variables to capture real-world data complexity such as multiplicative lighting, perspective transforms, triple synapses, or especially gating. In contrast, higher-order interactions could capture some of these interactions directly. Gating is a crucial, common operation in machine learning, as seen in LSTMs [37], GRUs [31], and attention networks. Third-order multiplicative interactions can be effectively viewed as soft gating operations thus provide more modeling power while remaining interpretable. Thus here we choose continuous graphical models with third-order interactions as a distribution family of high interest. Such distributions fall into the latter category of application where traditional models are infeasible but our GNNs could apply. Firstly, as a proof of concept, we construct two datasets of PGMs with known ground truth marginal distributions and closed-form BP update formulas so that we can compare the performance of our model with Belief Propagation. Second, we build a dataset of continuous PGMs with third-order interactions to test our model on this more complicated and interesting class of PGMs.

#### 3.4.1 Gaussian Graphical Model

As a toy example, we generate a dataset of random Gaussian Graphical Models (GGM). Since both marginalization and BP have closed-form solutions on GGMs, it becomes a convenient test for comparing our method with BP, and to test the generalization performance of our method to much larger out-of-distribution graphs.

We use the random graph generator algorithm WS-flex proposed in [38] to generate diverse graph structures parametrized by average shortest path length and cluster coefficient. To generate a random graph, we first sample the average degree  $k$  and rewiring probability  $p$  parameters for the WS-flex algorithm from a uniform distribution over  $[2, n-1]$  and  $[0, 1]$  where  $n$  is the number of variables, and then construct a random graph using these parameters. Each GGM has a precision matrix with non-zero entries randomly sampled by the WS-flex algorithm and eigenvalues uniformly drawn from  $[0.1, 10.0]$ . In order to achieve certain connectivity matrix with desired eigenvalues, we start from a positive-definite diagonal matrix, apply a random orthogonal rotation to make it dense, and then iteratively apply

Jacobi rotations to zero out elements according to the connectivity matrix until we achieve the desired structure. We concentrate on inferring the node variances and give all GGMs mean of zero, since the hard part of calculating both marginal means and variances is the inversion of the precision matrix.

### 3.4.2 Binary third-order factor graph

Our method works with general factor graphs, especially those with higher-order interactions, but GGMs have only pairwise interactions and can also be modeled by regular GNNs. To test our model on graphs with higher-order factors, we construct a dataset composed of binary graphical models with only third-order interactions. For the sake of exact solutions of marginal probabilities, we choose small binary spin glass models whose structures and connectivity strengths are randomly sampled so that exact marginal probabilities can be calculated by brute-force enumeration. The joint probability mass function is expressed as

$$p(\{\mathbf{s}\}) \propto \exp \left( \beta \left( \sum_{p=1}^3 \sum_{i \in \mathbb{I}_V} b_{i,p} s_i^p + \sum_{(ijk) \in \mathcal{N}(\mathcal{F})} J_{ijk} s_i s_j s_k \right) \right) \quad (13)$$

$\mathcal{N}(\mathcal{F})$  is the set of neighbor variable indices for each factor. We generate these random factor graphs using a generalization of the WS-flex generator, parameterized by average variable node degree  $k_3$  and rewiring probability  $p$ . Details of the algorithm could be found in the supplementary material. The singleton potential coefficients  $b_i^p$  and 3-way coupling coefficients  $J_{ijk}$  are randomly drawn from a standard Gaussian distribution and the inverse temperature,  $\beta$ , is chosen to be 0.5.

### 3.4.3 Continuous third-order factor graph

We are interested in continuous graphical models with third-order interactions, and we propose to use our method as an approximate inference algorithm for this model class. We construct a dataset of random continuous PGMs with third-order interactions and evaluate the accuracy of our message-passing algorithm against an expensive sampling approach. For each inference problem, a factor graph is randomly constructed such that 3-factors are generated using the aforementioned WS-flex variant, and 2-factors are generated using the regular WS-flex algorithm. Each graph structure is parametrized by three numbers: the average outdegree of variable nodes to 2-factor nodes  $k_2$ , the average outdegree of variable nodes to 3-factor nodes  $k_3$ , and the rewiring probability  $p$ .  $k_2$  is uniformly sampled from  $[2, n-1]$ ,  $k_3$  is uniformly sampled from  $[2, \lfloor (n-1)(n-2)/6 \rfloor]$ , and  $p$  is uniformly sampled from  $[0, 1]$ . An isotropic 4th-order base measure is added to ensure the joint density is normalizable:

$$p(\mathbf{x}) \propto \exp \left[ -\beta \left( \sum_{p=1}^3 \sum_{i \in \mathbb{I}_V} b_{i,p} x_i^p + \sum_{(ij) \in \mathcal{N}(\mathcal{F}_2)} K_{ij} x_i x_j + \sum_{(ijk) \in \mathcal{N}(\mathcal{F}_3)} J_{ijk} x_i x_j x_k + \alpha \|\mathbf{x}\|_{\ell_4}^4 \right) \right] \quad (14)$$

Bias parameters  $\{b_{i,p}\}$  and interaction strengths  $\{K_{ij}\}, \{J_{ijk}\}$  are sampled from a standard normal distribution  $\mathcal{N}(0, 1)$ . The strength of the 4th-order term and the inverse temperature were  $\alpha = 1.0$  and  $\beta = 0.3$ . Note that this exponential family of distributions is not closed under marginalization: marginals are not in the same family as the joint.

We run an MCMC algorithm, the No-U-Turn Sampler (NUTS) [39], using the Stan [40, 41] software for a large number of steps as an approximate ground truth. Our readout targets are summary statistics computed from those generated samples. For each random structure generated, we run 8 MCMC chains with 10000 warmup steps and 10000 sampling step each for a random set of parameter values and keep drawing new parameters until the potential scale reduction factor (PSRF) [42] falls below 1.2, indicating convergence has been reached for the MCMC chains. Here we choose the first four central moments as our targets since the Jensen-Shannon divergence between the empirical sample distribution and corresponding moment-matched maximum-entropy distribution does not decrease substantially when including more moments. fig. 1 shows random examples of sampled univariate marginals, the corresponding singleton distributions obtained by ignoring all multivariate interactions, and their maximum entropy counterparts by matching the first four central moments.

## 3.5 Training

We implement our models<sup>1</sup> in PyTorch [43] and PyTorch Geometric [44] and perform all experiments on internal clusters equipped with NVIDIA GTX 1080Ti and Titan RTX GPUs. We randomly split each dataset into a training and a validation set of ratio 4:1. The testing sets are constructed separately for different graph sizes. In every experiment, we use the ADAM [45] optimizer with batch size 100 and initial learning rate 0.001. We multiply the learning rate by

<sup>1</sup>Code is at <https://github.com/fy0cc/factor-inference-net/>

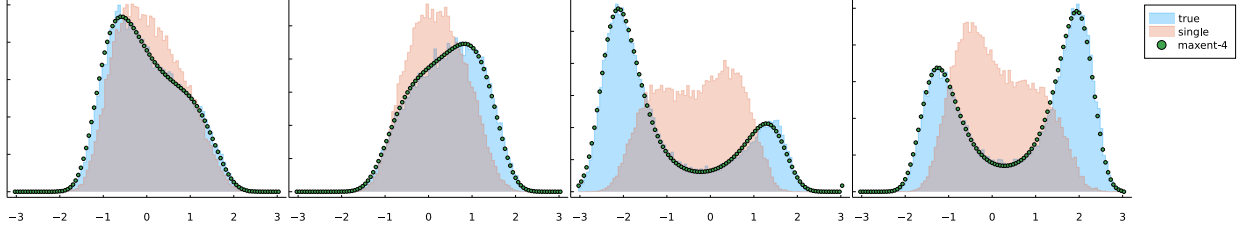


Figure 1: Example univariate marginal distributions from the continuous 3rd-order dataset. Shaded blue curves represents empirical marginal distributions from samples. Shaded orange curves are empirical single-variate distributions by only considering singleton potentials. Green dots represent the maximum entropy fit of the sample marginal distributions by matching first four central moments.

a factor of 0.2 if there is no improvement in 20 epochs, and perform early-stopping if there is no improvement in 40 epochs. We choose the dimension of hidden states for both variable and factor nodes  $\mathbf{h}_v, \mathbf{h}_f$  to be 64, and 5 attention heads are used for all experiments. For the encoder and decoder MLPs, we insert a BatchNorm [46] layer after the input layer and each hidden layer. We use mean-squared error (MSE) as loss on single-variate marginal precision values for the Gaussian dataset and on the first four central moments calculated from MCMC samples for the continuous third-order factor graph dataset respectively. As of the the binary spin-glass dataset, we use binary cross entropy as loss.

## 4 Experiments and Results

All GNNs are trained on graphs with size 10 solely, but are tested on graphs of various sizes. We uniformly draw the number of recurrent steps  $N$  from  $[30, 50]$ .  $N$  is set as 30 during testing. We repeat all experiments 10 times from different random seeds and report the mean and standard error on a held-out test set in table 1. Additionally, for each dataset, we pick the GNN with the lowest validation error among 10 run, and then compare their in-sample and out-of-sample error against BP in the space of graph metrics. As a baseline to show how strong the interactions are in each dataset, we also train a separate GNN (singleton GNN) that tries to predict the same target, but only sees singleton factors in the graphical model. Singleton GNN would have lower performance on graphs whose marginal distributions are strongly affected by multivariate interactions. Results of BP, full GNN, and singleton GNN are shown in fig. 2. Each point along with its error bar represents the bootstrapped mean and 95% confidence interval of the mean calculated from 100 resampling of the corresponding test set. Some error bars may be too small to see.

### 4.1 Gaussian Graphical Models

#### 4.1.1 Loopy Graphs

In this experiment we tested the performance of our model on Gaussian Graphical Models with zero mean, random precision matrices, and various structures generated as described in section 3.4.1. For a single GGM, the inverse variance of each variable’s marginal Gaussian distribution is used as target for supervised learning. 10000 random graphs with 10 variables are generated as a training dataset. Additionally, we generate various testing datasets with 10 to 50 variables, each consisting of 2000 random graphs. fig. 2(b), shows that our model trained on a dataset of GGMs with 10 variables has average KL divergence 6-fold smaller than Belief Propagation on a in-sample test set. When generalizing to larger graphs, our model still has smaller error than BP on graphs up to 30 variables. Other metrics, including  $R^2$  score and MSE (the training objective), are also shown in fig. 2(a)(c). Since BP doesn’t always converge on loopy graphs, all metrics are calculated on the subset of test graphs with convergent BP dynamics, which compose 73.2% to 71.2% of test set as graph size varies from 10 to 50. BP is considered non-convergent if the absolute error of beliefs between two adjacent BP updates still exceeds  $10^{-5}$  after 1000 cycles.

It is well known that Belief Propagation becomes non-exact on loopy graphs. Here we empirically investigate how BP and GNN performance depends on the graph structure by examining graph metrics. We choose two independent structural features that quantify the loopiness of a graph: average shortest path length and cluster coefficient [14]. The former quantifies the average loop length between any two nodes, and the latter describes the small-world property of a graph. Graphs in the test set are binned into 10 equal bins according the the graph metric, and for each bin we report the bootstrapped mean and its 95% CI for BP and GNN performance metrics (fig. 2(d-g)). Many real-world graphs have a small average path length and a large cluster coefficient [14], and this is the region where our model outperforms BP.

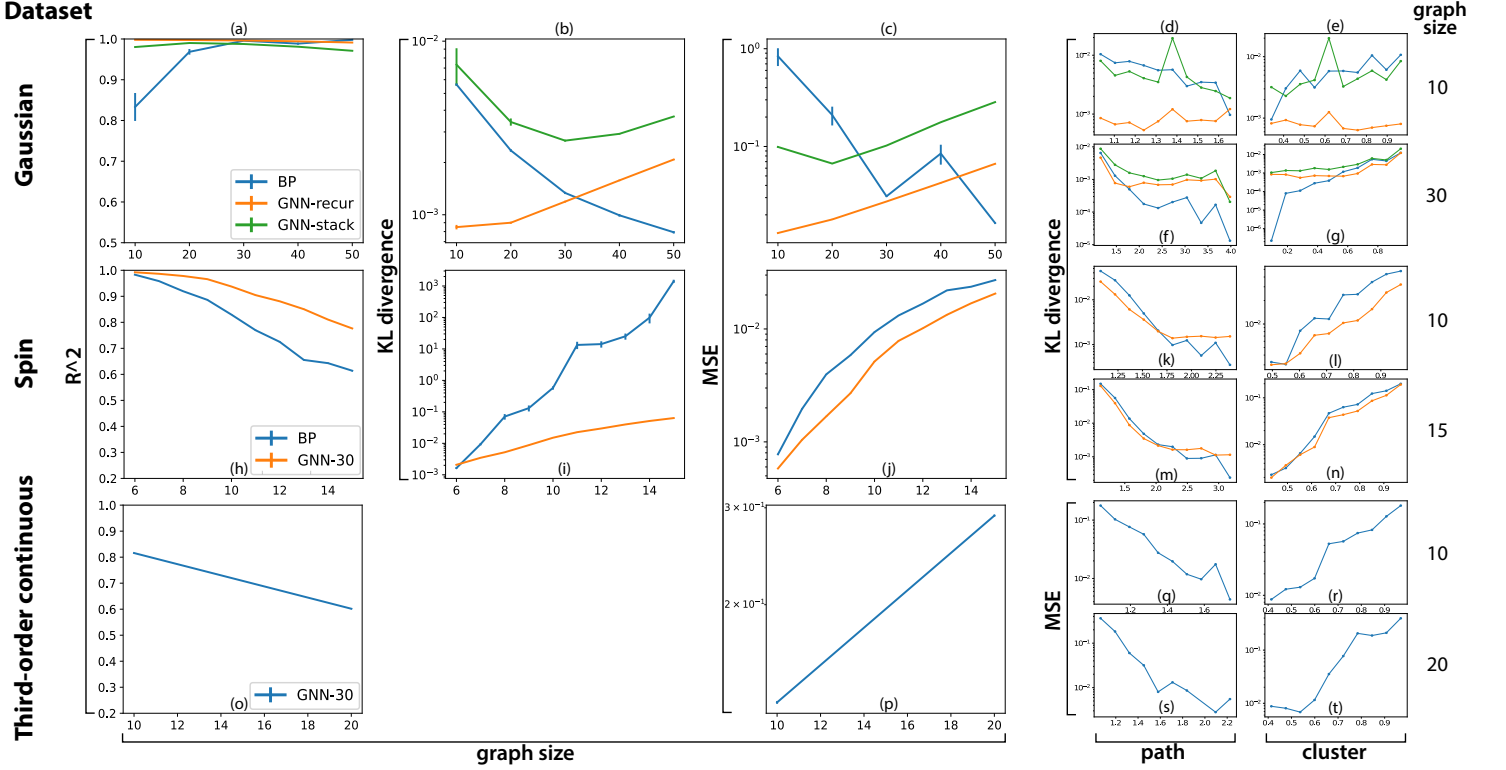


Figure 2: Performance on Gaussian, third-order spin, and third-order continuous datasets. Each row shows results of one dataset. In the first three columns, we compare the generalization performance of GNN and BP to larger graphs. All GNNs are trained on graphs with size 10. We also consider an additional 10-layer stacked GNN for the Gaussian dataset as a comparison. Three metrics- $R^2$ , KL divergence and MSE-are shown for the Gaussian and spin datasets. KL divergence is not available for the third-order continuous dataset thus omitted. Column 4 and 5 show how error of different methods depends on graph structures. We plot error against the average shortest path length in column 4, and against cluster coefficient in column 5. For each dataset, we show the in-sample results in the first row and generalization results on larger graphs in the second row.

BP can be viewed as an algorithm that finds local minima of the Bethe free energy by iteratively update messages until convergence [47]. Similarly, we also define our algorithm to be recursive. However, as comparison, we also constructed a feedforward model with 10 Factor-GNN layers stacked together. fig. 2(a-g) and table 1 shows that although the feedforward model has almost 10 times more parameters, the performance is worse than the recurrent one.

#### 4.1.2 Tree Graphs

BP is exact on tree graphs, so we also trained a model with a dataset of 10000 Gaussian tree graphs with size 10 using the eigenvalue distribution in section 3.4.1. A random tree structure is constructed by converting from a random Prüfer sequence [48], which is sampled uniformly from the symmetry group  $S_{n-2}$  where  $n$  is the number of nodes in the tree. BP is exact on trees with zero error, but our model also achieves excellent generalization performance with an in-distribution  $R^2$  score  $0.9995 \pm 0.0001$  and out-of-sample  $R^2$  score  $0.9996 \pm 0.0002$  even when generalizing to graphs with size 50.

#### 4.2 Spin systems with third-order interactions

For the binary spin systems with only third-order interactions and no pairwise interactions, we train our model on a dataset of size 10 and test on graphs with sizes from 6 to 15. We didn't test on larger graphs because it becomes impractical to enumerate all spin configurations in order to compute exact marginal probabilities. For binary graphical models, unlike in 4.1, non-convergent BP dynamics won't diverge, but may oscillate. Thus we take the beliefs from the last cycle if the dynamics does not converge in 1000 cycles. There is no qualitative difference when evaluating model performance using the whole test dataset or just BP-convergent ones, so we report the metrics on BP-convergent

Table 1: Experiment results on 4 PGM datasets

metric	dataset				
	method	GGM-tree	GGM-all	3rd-order binary	3rd-order continuous
KL	BP	<b>0</b>	0.0065	0.0269	N/A
	GNN	$0.0013 \pm 0.0004$	<b>0.0051</b> $\pm 0.0008$	<b>0.0152</b> $\pm 0.0005$	N/A
	Singleton	N/A	$0.0460 \pm 0.0001$	$0.0528 \pm 0.0000$	N/A
MSE	BP	<b>0</b>	0.1416	0.0094	N/A
	GNN	$0.0044 \pm 0.0013$	<b>0.0705</b> $\pm 0.0128$	<b>0.0057</b> $\pm 0.0002$	$0.0498 \pm 0.0009$
	Singleton	NA	$0.9027 \pm 0.0006$	$0.0215 \pm 0.0000$	$0.1930 \pm 0.0000$
$R^2$	BP	<b>1</b>	0.9719	0.8290	N/A
	GNN	$0.9995 \pm 0.0001$	<b>0.9876</b> $\pm 0.0023$	<b>0.9311</b> $\pm 0.0014$	$0.9107 \pm 0.0017$
	Singleton	N/A	$0.8329 \pm 0.0000$	$0.7352 \pm 0.0000$	$0.6543 \pm 0.0001$

graphs to maintain consistency with 4.1. Within the range of testing graphs, our model consistently outperforms BP on average (fig. 2(h-j)). In the space of graph structures parametrized by average shortest path length and cluster coefficient, our model performs better than BP in regions with smaller average shortest path length and larger cluster coefficient, which agrees with the result of section 4.1 (fig. 2(k-n)).

### 4.3 Continuous third-order graphical model

For general continuous non-Gaussian graphical models it is not feasible to compare our method with BP because the BP message update neither an explicit formula, nor could be calculated exactly by enumeration. Even the EP message update needs to be approximated [15, 16, 17]. Like these approximation methods, we also train a predictor to calculate approximate marginal distributions. However, instead of approximating the EP message-passing for a specific type of factors within the EP framework, we learn a new message-passing algorithm end-to-end that works with many factor types and doesn't share EP's limitations. This approach is more applicable to loopy graphs where BP and EP struggle.

For this experiment we constructed a continuous graphical model with third-order interactions and train our model to predict the first four central moments of every univariate marginal distribution (see Section 3.4.3). Since BP or EP is not feasible for this dataset, we only compare our model with the singleton GNN as our baseline. A model trained on graphs with 10 variables achieves an in-sample  $R^2$  score of  $0.911 \pm 0.005$ , while the baseline model without interactions has an  $R^2$  of only  $0.654 \pm 0.001$ . We test the generalization performance of our model with a dataset of graphs of size 20. For the MCMC algorithm to produce convergent chains, we shrink the interaction strengths by a factor of 2 but keep the singleton parameter distribution unchanged so that both input and output values fall in the training ranges. On a test set of 1000 graphs, the full model has an  $R^2$  score of  $0.582 \pm 0.021$ , while the baseline model has an  $R^2$  score of  $0.495 \pm 0.000$ . Qualitatively similar to the Gaussian and spin dataset, model performance drops when generalizing to larger graphs (fig. 2(o-p)), and our model has larger error on loopy graphs (fig. 2(q-t)) since these are hard ones.

## 5 Discussion

In this paper we show that GNN is an alternative to traditional message-passing algorithms like Belief Propagation as an approximate inference engine on graphical models. It outperforms BP on some loopy graphs, and offers a practical way to perform fast inference for continuous non-Gaussian graphical models like those in 4.3. In contrast, previous data-driven methods [49, 15, 17] were proposed to approximate the EP message passing for a single factor type, thus still shares the weakness of EP on loopy graphs.

Although our method achieves promising results and does generalize to graphs of different sizes, it naturally performs better within its training distribution. However, almost no performance drop on Gaussian tree graphs when generalizing to 5x larger graphs (section 4.1.2 and promising generalization results on loopy graphs (section 4.1.1, section 4.2)) suggest the potential usage of our methods for inference on large graphs by training on smaller ones. Compared to a 10-layer stacked GNN 2, our method achieves better performance with substantially fewer parameters. However, in our experiment we just simply stack the Factor-GNN layers with out any further tricks like skip connection, pooling layer, etc., as in [18]. Despite that, learning a recursive message-passing algorithm has advantages over a feedforward one when generalizing to larger graphs: the number of layers must scale with graph size for a feedforward network in order to distribute information throughout the graph, whereas a recurrent algorithm could run until convergence regardless of the graph size.



A limitation of our method is that a separate GNN needs to be learnt from scratch whenever encountering a new parametric family of graphical models. One exciting but speculative possibility is to extend this framework such that whenever a new type of factor is encountered, the model only trains a dedicated new encoder/decoder, and reuses a shared core message-passing module, perhaps implementing a more universal inference engine akin to a shared language model [50]. This can be useful when data is limited, since the difficult message-passing core could be learnt from multiple rich datasets. The general form of Belief Propagation takes this universal form, and have some multifactor extensions like Generalized BP [51]. We hypothesize that Factor Graph Neural Networks could potentially extend this universality while compensating for the challenges of inference in a loopy world.

Creation of smarter artificial intelligence would have major impacts on human life, through communication, industry, infrastructure, robotics, and many more aspects of life. Our work aims to refine the theoretical foundations for intelligence. Thoughtless or naive application of these scientific advances could lead to unanticipated consequences and increase social inequality.

## 6 Acknowledgements

The authors thank Kijung Yoon for helpful conversations about graph metrics. YF and XP were supported in part by NSF NeuroNex grant 1707400. XP was supported in part by NSF CAREER award 1552868 and a grant from the McNair Foundation.

## References

- [1] Daphne Koller and Nir Friedman. *Probabilistic graphical models: principles and techniques*. MIT press, 2009.
- [2] Judea Pearl. *Probabilistic reasoning in intelligent systems: networks of plausible inference*. Morgan Kaufmann, 1988.
- [3] Thomas P Minka. Expectation propagation for approximate bayesian inference. In *Proceedings of the Seventeenth conference on Uncertainty in artificial intelligence*, pages 362–369. Morgan Kaufmann Publishers Inc., 2001.
- [4] John J Hopfield. Neural networks and physical systems with emergent collective computational abilities. *Proceedings of the national academy of sciences*, 79(8):2554–2558, 1982.
- [5] David Sherrington and Scott Kirkpatrick. Solvable model of a spin-glass. *Physical review letters*, 35(26):1792, 1975.
- [6] John M Beggs and Dietmar Plenz. Neuronal avalanches in neocortical circuits. *Journal of neuroscience*, 23(35):11167–11177, 2003.
- [7] Elad Ganmor, Ronen Segev, and Elad Schneidman. Sparse low-order interaction network underlies a highly correlated and learnable neural population code. *Proceedings of the National Academy of Sciences*, 108(23):9679–9684, 2011.
- [8] Hideaki Shimazaki, Kolia Sadeghi, Tomoe Ishikawa, Yuji Ikegaya, and Taro Toyoizumi. Simultaneous silence organizes structured higher-order interactions in neural populations. *Scientific reports*, 5(1):1–13, 2015.
- [9] Terrence J Sejnowski. Higher-order boltzmann machines. In *AIP Conference Proceedings*, volume 151, pages 398–403. American Institute of Physics, 1986.
- [10] Roland Memisevic and Geoffrey E Hinton. Learning to represent spatial transformations with factored higher-order boltzmann machines. *Neural computation*, 22(6):1473–1492, 2010.
- [11] F Scarselli, M Gori, and Tsoi -AC Networks. The graph neural network model. 2009.
- [12] Yujia Li, Daniel Tarlow, Marc Brockschmidt, and Richard Zemel. Gated graph sequence neural networks. *arXiv preprint arXiv:1511.05493*, 2015.
- [13] KiJung Yoon, Renjie Liao, Yuwen Xiong, Lisa Zhang, Ethan Fetaya, Raquel Urtasun, Richard Zemel, and Xaq Pitkow. Inference in Probabilistic Graphical Models by Graph Neural Networks. 03 2018.
- [14] Duncan J Watts and Steven H Strogatz. Collective dynamics of ‘small-world’ networks. *nature*, 393(6684):440–442, 1998.
- [15] Nicolas Heess, Daniel Tarlow, and John Winn. Learning to Pass Expectation Propagation Messages. page 3219 3227, 2013.
- [16] S M Ali Eslami, Daniel Tarlow, Pushmeet Kohli, and John Winn. Just-In-Time Learning for Fast and Flexible Inference. page 154 162, 2014.

- [17] Wittawat Jitkrittum, Arthur Gretton, Nicolas Heess, S M Ali Eslami, Balaji Lakshminarayanan, Dino Sejdinovic, and Zoltán Szabó. Kernel-Based Just-In-Time Learning for Passing Expectation Propagation Messages. 03 2015.
- [18] Zhen Zhang, Fan Wu, and Wee Sun Lee. Factor Graph Neural Network. *arXiv.org*, cs.LG, 06 2019.
- [19] Petar Veličković, Guillem Cucurull, Arantxa Casanova, Adriana Romero, Pietro Liò, and Yoshua Bengio. Graph Attention Networks. 10 2017.
- [20] Victor Garcia Satorras and Max Welling. Neural Enhanced Belief Propagation on Factor Graphs. *arXiv*, 2020.
- [21] Brendan J Frey, Frank R Kschischang, Hans-Andrea Loeliger, and Niclas Wiberg. Factor graphs and algorithms. In *Proceedings of the Annual Allerton Conference on Communication Control and Computing*, volume 35, pages 666–680. Citeseer, 1997.
- [22] Song Bai, Feihu Zhang, and Philip H S Torr. Hypergraph Convolution and Hypergraph Attention. *arXiv*, 2019.
- [23] Yiding Zhang, Xiao Wang, Xunqiang Jiang, Chuan Shi, and Yanfang Ye. Hyperbolic Graph Attention Network. 2019.
- [24] Christopher Morris, Martin Ritzert, Matthias Fey, William L Hamilton, Jan Eric Lenssen, Gaurav Rattan, and Martin Grohe. Weisfeiler and Leman Go Neural: Higher-Order Graph Neural Networks. *Proceedings of the AAAI Conference on Artificial Intelligence*, 33:4602–4609, 07 2019.
- [25] Stefania Ebli, Michaël Defferrard, and Gard Spreemann. Simplicial Neural Networks. *arXiv*, 2020.
- [26] Christopher M. Bishop. *Pattern Recognition and Machine Learning*. Springer, 2006.
- [27] Jie Zhou, Ganqu Cui, Shengding Hu, Zhengyan Zhang, Cheng Yang, Zhiyuan Liu, Lifeng Wang, Changcheng Li, and Maosong Sun. Graph neural networks: A review of methods and applications. *AI Open*, 1:57–81, 2020.
- [28] Thomas N Kipf and Max Welling. Semi-Supervised Classification with Graph Convolutional Networks. *arXiv.org*, cs.LG, 09 2016. Published as a conference paper at ICLR 2017.
- [29] Marco Gori, Gabriele Monfardini, and Franco Scarselli. A new model for learning in graph domains. In *Neural Networks, 2005. IJCNN’05. Proceedings. 2005 IEEE International Joint Conference on*, volume 2, pages 729–734. IEEE, 2005.
- [30] Martin J Wainwright, Tommi S Jaakkola, and Alan S Willsky. Tree-based reparameterization framework for analysis of sum-product and related algorithms. *IEEE Transactions on information theory*, 49(5):1120–1146, 2003.
- [31] Kyunghyun Cho, Bart van Merriënboer, Caglar Gulcehre, Dzmitry Bahdanau, Fethi Bougares, Holger Schwenk, and Yoshua Bengio. Learning phrase representations using RNN encoder–decoder for statistical machine translation. In *Proceedings of the 2014 Conference on Empirical Methods in Natural Language Processing (EMNLP)*, pages 1724–1734. Association for Computational Linguistics, 2014.
- [32] Jimmy Lei Ba, Jamie Ryan Kiros, and Geoffrey E Hinton. Layer Normalization. *arXiv*, 2016.
- [33] E. J. G. Pitman. Sufficient statistics and intrinsic accuracy. *Mathematical Proceedings of the Cambridge Philosophical Society*, 32(4):567–579, 1936.
- [34] B. O. Koopman. On distributions admitting a sufficient statistic. *Transactions of the American Mathematical Society*, 39(3):399–409, 1936.
- [35] Martin J. Wainwright and Michael I. Jordan. Graphical models, exponential families, and variational inference - compressed. 2008.
- [36] Justin Gilmer, Samuel S Schoenholz, Patrick F Riley, Oriol Vinyals, and George E Dahl. Neural message passing for Quantum chemistry. page 1263 1272, 04 2017.
- [37] Sepp Hochreiter and Jürgen Schmidhuber. Long short-term memory. *Neural computation*, 9(8):1735–1780, 1997.
- [38] Jiaxuan You, Jure Leskovec, Kaiming He, and Saining Xie. Graph Structure of Neural Networks. *arXiv*, 2020.
- [39] Matthew D Hoffman and Andrew Gelman. The no-u-turn sampler: adaptively setting path lengths in hamiltonian monte carlo. *J. Mach. Learn. Res.*, 15(1):1593–1623, 2014.
- [40] Stan Development Team. The Stan Core Library, 2021. Version 2.26.0.
- [41] StanSample.jl. <https://github.com/StanJulia/StanSample.jl>, 2021. Version 3.0.11.
- [42] Andrew Gelman, Donald B Rubin, et al. Inference from iterative simulation using multiple sequences. *Statistical science*, 7(4):457–472, 1992.

- [43] Adam Paszke, Sam Gross, Francisco Massa, Adam Lerer, James Bradbury, Gregory Chanan, Trevor Killeen, Zeming Lin, Natalia Gimelshein, Luca Antiga, Alban Desmaison, Andreas Kopf, Edward Yang, Zachary DeVito, Martin Raison, Alykhan Tejani, Sasank Chilamkurthy, Benoit Steiner, Lu Fang, Junjie Bai, and Soumith Chintala. Pytorch: An imperative style, high-performance deep learning library. In H. Wallach, H. Larochelle, A. Beygelzimer, F. d’Alché Buc, E. Fox, and R. Garnett, editors, *Advances in Neural Information Processing Systems 32*, pages 8024–8035. 2019.
- [44] Matthias Fey and Jan E. Lenssen. Fast graph representation learning with PyTorch Geometric. In *ICLR Workshop on Representation Learning on Graphs and Manifolds*, 2019.
- [45] Diederik P Kingma and Jimmy Ba. Adam: A Method for Stochastic Optimization. *arXiv.org*, cs.LG, 12 2014. Published as a conference paper at the 3rd International Conference for Learning Representations, San Diego, 2015.
- [46] Sergey Ioffe and Christian Szegedy. Batch normalization: Accelerating deep network training by reducing internal covariate shift. In *International conference on machine learning*, pages 448–456. PMLR, 2015.
- [47] Tom Heskes et al. Stable fixed points of loopy belief propagation are minima of the bethe free energy. *Advances in neural information processing systems*, 15:359–366, 2003.
- [48] Heinz Prüfer. Neuer beweis eines satzes über permutationen. *Arch. Math. Phys*, 27(1918):742–744, 1918.
- [49] Simon Barthelmé and Nicolas Chopin. Abc-ep: expectation propagation for likelihoodfree bayesian computation. In *ICML*, 2011.
- [50] Michael Denkowski and Alon Lavie. Meteor universal: Language specific translation evaluation for any target language. In *Proceedings of the ninth workshop on statistical machine translation*, pages 376–380, 2014.
- [51] Jonathan S Yedidia, William T Freeman, Yair Weiss, et al. Generalized belief propagation. In *NIPS*, volume 13, pages 689–695, 2000.

## Supplementary Materials

### S.7 Random factor graph generator for 3-factors

We use the WS-flex[38] variant algorithm to generate a random factor graph with only 3-factors. This includes two stages: generating a ring-like factor graph, and rewiring. In the first stage, given average variable node degree  $k$  and number of variable nodes  $n$ , the number of factors is  $f = \lfloor nk/3 \rfloor$ . On average there are  $\lfloor f/n \rfloor$  3-factors centered at each variable node. The other two legs of these factors are connected to the closest neighbors of the center variable, while keeping the factor unique. For example, three 3-factors centered at variable 5 may be connected to variables (4, 5, 6), (4, 5, 7) and (3, 5, 6) respectively. The remaining  $(f \bmod n)$  3-factors are then formed by randomly picking the center variable and choose the closest two neighbours, while avoiding redundant factors. After this ring is created, in a second stage we may rewire each factor with probability  $p$  by randomly picking three new neighbours without duplication.

### S.8 Additional figures: testing performance on graphs with various sizes

In the paper we show how GNN and BP perform with respect to two graph metrics: average shortest path length and cluster coefficient. Here we provide these two figures on testing sets with more sizes for the Gaussian dataset and the binary dataset.

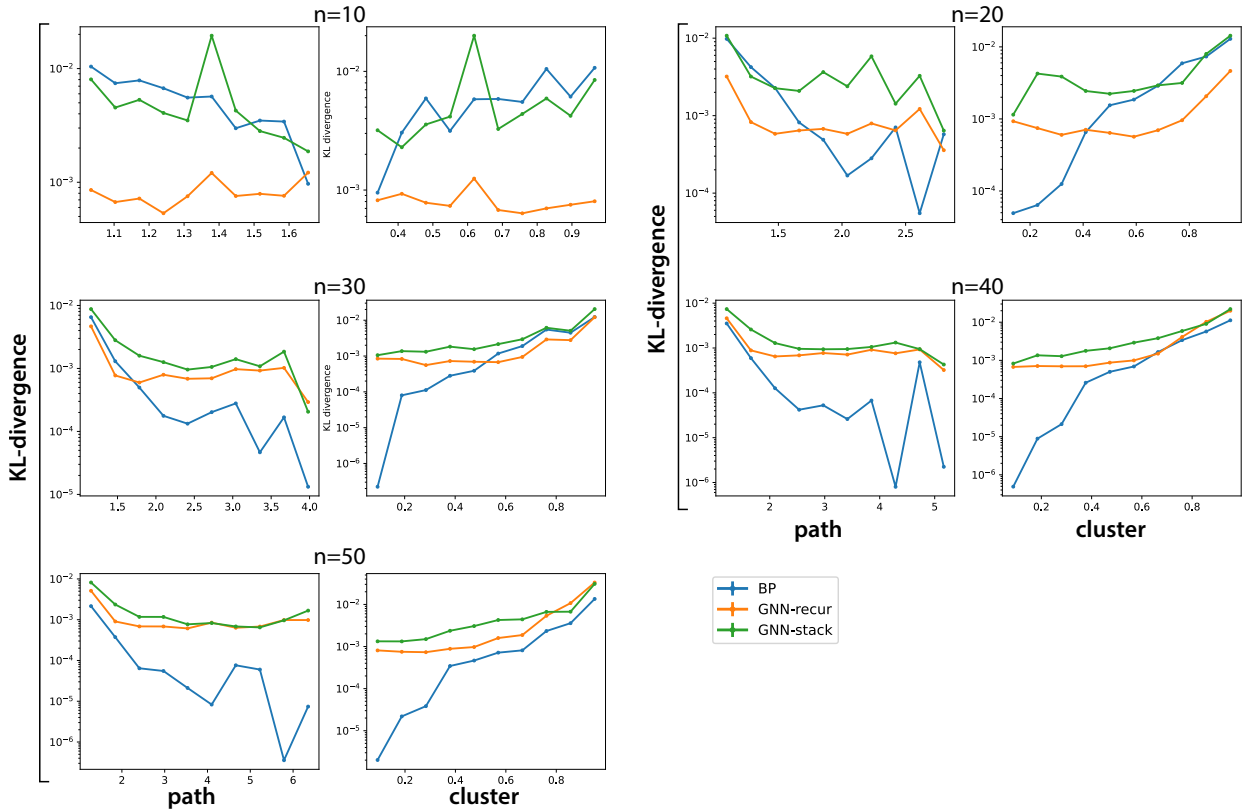


Figure S1: **Gaussian dataset:** dependence of KL divergence between true marginal distribution and model prediction on average shortest path length and cluster coefficient. We compare Belief Propagation (blue), recurrent Factor-GNN with GRU (orange), and 10-layer stacked Factor-GNN (green) respectively. The recurrent GNN and stacked GNN are trained on the same graphical models dataset with 10 variables. Each pair of panels shows the testing performance on a dataset with graphs of fixed size ranging from 10 to 50.

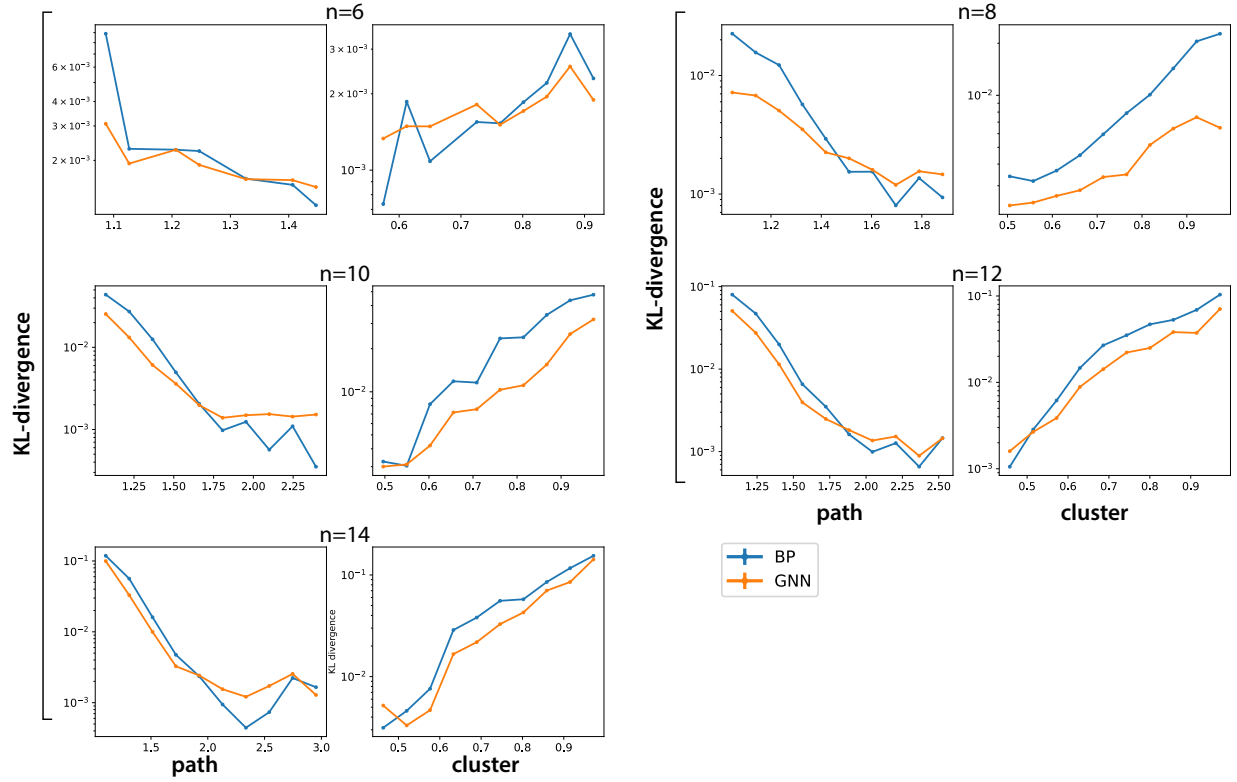


Figure S2: **Binary dataset:** dependence of KL divergence between true marginal distribution and model prediction on average shortest path length and cluster coefficient, plotted as in Supplemental Figure S1. Each pair of panels shows the testing performance on new graphical models with fixed numbers of variables ranging from 6 to 14.